Statistical production and binding energy of hypernuclei

N. Buyukcizmeci,[1] A. S. Botvina,[2,3] A. Ergun,[1] R. Ogul,[1] and M. Bleicher[2,4,5]

[1]*Department of Physics, Selcuk University, 42079 Kampus, Konya, Turkey*
[2]*FIAS and ITP J.W. Goethe University, D-60438 Frankfurt am Main, Germany*
[3]*Institute for Nuclear Research, Russian Academy of Sciences, 117312 Moscow, Russia*
[4]*GSI Helmholtz Center for Heavy Ion Research, Planckstr. 1, Darmstadt, Germany*
[5]*John-von-Neumann Institute for Computing (NIC), FZ Jülich, Jülich, Germany*

High-energy nuclear reactions enable us to produce a large variety of hypernuclei through the capture of hyperons by nuclear residues. We explore the statistical disintegration of such hypernuclear systems and the connection of fragment production to the binding energies of hyperons. It has been demonstrated that the hyperon binding energies can be effectively evaluated from the yields of different isotopes of hypernuclei by using the double ratio method. The advantages of this procedure are its universality and the possibility to involve many different isotopes. This method can also be applied for multistrange nuclei, for which binding energies were very difficult to measure in previous hypernuclear experiments. Corrections caused by secondary deexcitation processes are also discussed.

I. INTRODUCTION

A promising way to produce hypernuclei is to use the copious production of hyperons (Λ, Σ, Ξ, Ω) in relativistic nuclear reactions and their subsequent capture by nuclei, e.g.,, in the fragmentation region. Compared to the time scale of a heavy-ion reaction, hypernuclei can be considered stable. Baryons with strangeness embedded in the nuclear environment allow us to explore the many-body aspects of the strong three-flavor interaction (i.e., including u, d, and s quarks) at low energies. Hypernuclei can also serve as a tool to study the hyperon-nucleon and potentially the hyperon-hyperon interactions. The investigation of reactions leading to the formation of hypernuclei and the structure of hypernuclei have been a growing field of nuclear physics. It provides a complementary method to improve traditional nuclear studies and opens new horizons for studying particle physics and nuclear astrophysics (see, e.g., Refs. [1–6] and references therein).

Traditionally, hypernuclear physics has been focused mainly on spectroscopic information and restricted by a quite limited set of lepton- and hadron-induced reactions [1,2]. In these reactions the hyperons produced in the first interaction are directly captured by nuclei in their ground states and low excited states. Kaons have often been used for tagging this production channel. Within this method it was possible to obtain the binding energies of hyperons inside nuclei by measuring nearly all products of the reaction exactly. However, there are severe limitations on such methods, since the targets should be mainly stable (not radioactive). Therefore many hypernuclear isotopes are not reachable experimentally in this case.

We emphasize another possibility to form hypernuclei in the relativistic deep-inelastic reactions leading to fragmentation processes, as they were discovered long ago [7]. One can form hypernuclei of all sizes and isospin content when these hyperons are captured by nucleons and nuclear fragments produced in the same reaction events. Many experimental collaborations (STAR at RHIC [8], ALICE at LHC [9], PANDA [10], CBM [11], HypHI, Super-FRS, R3B at FAIR [12,13], BM@N, MPD at NICA [14]) plan to investigate hypernuclei and their properties in reactions induced by relativistic hadrons and ions. The limits in isospin space, particle unstable states, multiple strange nuclei and precise lifetime measurements are unique topics of these fragmentation reactions. A capture of hyperons by large nuclear residues is especially interesting since it provides a natural way to study large bulbs of hypermatter and its evolution, for example, the liquid-gas-type phase transition. It was theoretically demonstrated [5,15–21] that in such a way it is possible to produce all kinds of hypernuclei including multistrange ones. There were also experimental confirmations of such processes leading to hypernuclei [12,22,23].

Below, we consider deep-inelastic reaction processes caused by relativistic projectiles in nuclear matter leading to abundant production of hyperons in primary and secondary hadron collisions. In the following we take into account the capture of these hyperons by the matter with producing hypermatter in chemical equilibrium. This is a typical situation for fragmentation and multifragmentation reactions initiated in relativistic peripheral nucleus-nucleus collisions, as well as in high-energy hadron/lepton reactions on large targets. The possibility to obtain many kinds of hypernuclei in the same reaction opens new opportunities for their investigation in comparison with previous methods. Complex multihypernuclear systems incorporating more than two hyperons can be created in the energetic nucleus-nucleus collisions [16,19]. This may be the only conceivable method to go beyond

064603-1

double hypernuclei, and obtain new experimental information on properties of multihyperon systems. In this paper we continue the theoretical investigation of this kind of reaction and propose a new double ratio method demonstrating how the important knowledge on the hyperon binding energies, including in multistrange nuclei, can be extracted from the analyses of relative yields of hypernuclei.

II. STATISTICAL PRODUCTION OF HYPERNUCLEI FROM EXCITED HYPERNUCLEAR SYSTEMS

The hyperons are abundantly produced in high-energy particle reactions, e.g., nucleus-nucleus, hadron-nucleus, and lepton-nucleus collisions. This production of strangeness correlates with particle production and it is usually accompanied by many nucleons emission within such explosive events. An initial nucleus can lose many nucleons, and, as known from normal nucleus interactions, these processes can lead to a high excitation of remaining residual nuclei, see, e.g., Refs. [24–26]. Therefore, the capture of a produced hyperon will be also realized mostly at the excited nuclei. As a result, such deep-inelastic processes can form large hyperresidues with very broad distribution in mass and excitation energy. As was demonstrated in our previous works [17–19], the yields of the hypernuclear residues in peripheral ion collisions will saturate with energies above 3–5 A GeV (in the laboratory frame).

The reactions of formation of excited nuclear residues in high-energy nucleus-nucleus and hadron-nucleus collisions were intensively studied in connection with fragmentation and multifragmentation processes. In particular, masses and excitation energies of the residues are known from experimental and theoretical works, e.g., Refs. [19,25]. At high excitation energies, the dominating decay mode is corresponding to a multifragmentation process [24,27,28]. The interactions of a hyperon in a nucleus are similar to normal nuclear ones, and its potential is expected to be around two-thirds of the nucleon potential. Therefore, the general picture of disintegration reactions with a large energy deposition in a big piece of nuclear matter does not change in the presence of few hyperons. According to the present understanding, multifragmentation is a relatively fast process, with a characteristic time around 100 fm/c, where, nevertheless, a high degree of equilibration (chemical equilibrium) is reached. This is a consequence of the strong interaction between baryons located in the vicinity of each other in the freeze-out volume.

The statistical models have demonstrated very good agreement with fragmentation and multifragmentation data [24,25,27,29]. It is naturally to extend the statistical approach for hypernuclear systems. It is also instructive that the same numerical methods used previously for execution of the models can be extended. The statistical multifragmentation model (SMM), which was very successfully applied for description of normal multifragmentation processes, was generalized for hypernuclei in Ref. [15]. A transition from the compound hypernucleus to the multifragmentation regime was also under investigation [5,15]. In the SMM, the break-up channels are generated according to their statistical weight. The grand canonical approximations leads to the following

average yields of individual fragments with the mass (baryon) number A, charge Z, and the Λ-hyperon number H:

$$Y_{A,Z,H} = g_{A,Z,H} \cdot V_f \frac{A^{3/2}}{\lambda_T^3} \exp\left[-\frac{1}{T}(F_{A,Z,H} - \mu_{AZH})\right],$$

$$\mu_{AZH} = A\mu + Z\nu + H\xi. \tag{1}$$

Here T is the temperature, $F_{A,Z,H}$ is the internal free energies of these fragments, V_f is the free volume available for the translation motion of the fragments, $g_{A,Z,H}$ is the spin degeneracy factor of species (A, Z, H), $\lambda_T = (2\pi\hbar^2/m_N T)^{1/2}$ is the baryon thermal wavelength, m_N is the average baryon mass. The chemical potentials μ, ν, and ξ are responsible for the mass (baryon) number, charge, and strangeness conservation in the system, and they can be numerically found from the corresponding conservation laws accounting for the total baryon number A_0, the total charge Z_0, and the total hyperon number H_0 in the system. In this model the statistical ensemble includes all break-up channels composed of baryons and excited fragments. The primary fragments are formed in the freeze-out volume V. We use the excluded volume approximation $V = V_0 + V_f$, where $V_0 = A_0/\rho_0$ ($\rho_0 \approx 0.15$ fm^{-3} is the normal nuclear density), and parametrize the free volume $V_f = \kappa V_0$, with $\kappa \approx 2$, as taken in description of experiments in Refs. [25,27,29].

The following model prescriptions depend on the physical processes, which are the most adequate to the analyzed reactions. In many cases nuclear clusters in the freeze-out volume can be described in the liquid-drop approximation: Light fragments with mass number $A < 4$ are treated as elementary particles with corresponding spins and translation degrees of freedom (nuclear gas). Their binding energies were taken from experimental data [1,2,24]. The fragments with $A = 4$ are also treated as gas particles with table masses, however, some excitation energy is allowed $E_x = AT^2/\varepsilon_0$ ($\varepsilon_0 \approx 16$ MeV is the inverse volume level density parameter [24]), that reflects a presence of excited states in ^{4}He, $^4_\Lambda$H, and $^4_\Lambda$He nuclei. Fragments with $A > 4$ are treated as heated liquid drops. In this way one can study the nuclear liquid-gas coexistence of hypermatter in the freeze-out volume. The internal free energies of these fragments are parametrized as the sum of the bulk (F_A^B), the surface (F_A^S), the symmetry (F_{AZH}^{sym}), the Coulomb (F_{AZ}^C), and the hyperenergy (F_{AH}^{hyp}):

$$F_{A,Z,H} = F_A^B + F_A^S + F_{AZH}^{\text{sym}} + F_{AZ}^C + F_{AH}^{\text{hyp}}. \tag{2}$$

Here, the first three terms are written in the standard liquid-drop form [24]:

$$F_A^B = \left(-w_0 - \frac{T^2}{\varepsilon_0}\right)A, \tag{3}$$

$$F_A^S = \beta_0\left(\frac{T_c^2 - T^2}{T_c^2 + T^2}\right)^{5/4} A^{2/3}, \tag{4}$$

$$F_{AZH}^{\text{sym}} = \gamma \frac{(A - H - 2Z)^2}{A - H}, \tag{5}$$

where $w_0 = 16$ MeV, $\beta_0 = 18$ MeV, $T_c = 18$ MeV, and $\gamma = 25$ MeV are the model parameters, which are extracted from nuclear phenomenology and provide a good description of

multifragmentation data [24,25,27,29]. The Coulomb interaction of fragments is described within the Wigner-Seitz approximation, and F_{AZ}^C is taken as in the Refs. [15,24]:

$$F_{AZ}^C(V) = \frac{3}{5}\left[1 - \left(\frac{V_0}{V}\right)^{1/3}\right]\frac{(eZ)^2}{r_0 A^{1/3}}, \qquad (6)$$

where $r_0 = 1.2$ fm and e denotes the electron charge.

For our purpose the free hyperenergy term F_{AH}^{hyp} is very important. We assume that it is determined only by the binding energy of hyperfragments. Presently, only the masses of a few ten single hypernuclei (mostly light ones) are experimentally established [1,2], and only a few single-event measurements of double hypernuclei exist. Still, there are theoretical estimations of their masses including hyperon binding energies based on this limited amount of available data. In Ref. [15] we have suggested a liquid drop hyperterm:

$$F_{AH}^{\text{hyp}} = (H/A) \cdot (-10.68A + 21.27A^{2/3})\,\text{MeV}. \qquad (7)$$

Such a term is proportional to the share of hyperons in matter (H/A). The second part is the volume contribution minus the surface one, which is a normal liquid-drop parametrization assuming saturation of the nuclear interaction. The linear dependence at small H/A is in agreement with theoretical predictions [30] for hypermatter. As was demonstrated in Refs. [5,15] this parametrization of the hyperon free energy describes available experimental data on the hyperon separation energy quite reasonably. It is important that two boundary physical effects are correctly reproduced: The binding energies of light hypernuclei (if a hyperon substitutes a neutron) can be lower than in normal nuclei, since the hyperon-nucleon potential is smaller than the nucleon-nucleon one. However, since the hyperon can take the lowest s state, it can increase the nuclear binding energies, especially for large nuclei. There were also suggested other phenomenological hyperformulae (e.g., Ref. [31]), and their sensitivity for fragment production was under investigations [15].

III. DOUBLE RATIO METHOD FOR EVALUATION OF THE HYPERON BINDING

The advantage of the following suggested method [32] is that it does not depend on the theoretical assumptions on the nuclear hyperterms, e.g., formula (7), and is determined mainly by the fragment yields obtained in the reactions. The experimental information on hypernuclei is very limited, therefore, there is an urgent need to increase the number of known hypernuclei by involving new reactions for experimental measurements. The deep-inelastic fragmentation and multifragmentation reactions are very promising since they lead to the production of both strangeness and large fragments. One can also use different assumptions on fragment parameters in the statistical freeze-out state depending on the reaction/production mechanisms. As established in the analysis of normal multifragmentation experiments, there are methods to identify both nuclear fragments and the processes of their production in the same events. Within the statistical approaches we demonstrate below how the hypernuclei yields can be used for addressing the hyperon binding energies.

A. Standard multifragmentation picture

As the standard case we can use the formulas (1) and (2). It is convenient to rewrite the above statistical expressions in order to show separately the binding energy E_A^{bh} of one hyperon at the temperature T inside a hypernucleus with (A, Z, H) as follows:

$$E_A^{\text{bh}} = F_{A,Z,H} - F_{A-1,Z,H-1}. \qquad (8)$$

Since Λ hyperon is usually bound, this value is negative. Then the yield of hypernuclei with an additional Λ hyperon can be recursively written by using the former yields as follows:

$$Y_{A,Z,H} = Y_{A-1,Z,H-1} \cdot C_{A,Z,H} \cdot \exp\left[-\frac{1}{T}\left(E_A^{\text{bh}} - \mu - \xi\right)\right], \qquad (9)$$

where $C_{A,Z,H} = (g_{A,Z,H}/g_{A-1,Z,H-1}) \cdot (A^{3/2}/(A-1)^{3/2})$ depends mainly on the ratio of the spin factors of (A, Z, H) and $(A-1, Z, H-1)$ nuclei, and very weakly on A. Since we assume in the liquid-drop approximation that the fragments with $A > 4$ are excited and do populate many states above the ground ones according to the given temperature dependence of the free energy, then we take $g_{A,Z,H} = 1$. Within SMM we can connect the relative yields of hypernuclei with the hyperon binding energies. It is interesting that in this mathematical formulation one can use other parametrizations to describe nuclei in the freeze-out. This statistical approach is quite universal, and only small corrections such as the table-known spins and energies may be required for more extensive consideration.

We propose the following recipe for obtaining information on the binding energies of hyperons inside nuclei from the hypernuclei yields. Let us take two hypernuclei with different masses, (A_1, Z_1, H) and (A_2, Z_2, H), together with nuclei, which differ from them only by one Λ hyperon. We consider the double ratio (DR) of $Y_{A_1,Z_1,H}/Y_{A_1-1,Z_1,H-1}$ to $Y_{A_2,Z_2,H}/Y_{A_2-1,Z_2,H-1}$. Then, one can obtain from the above formulas

$$DR_{A_1 A_2} = \frac{Y_{A_1,Z_1,H}/Y_{A_1-1,Z_1,H-1}}{Y_{A_2,Z_2,H}/Y_{A_2-1,Z_2,H-1}}$$

$$= \alpha_{A_1 A_2}\exp\left[-\frac{1}{T}\left(\Delta E_{A_1 A_2}^{\text{bh}}\right)\right], \qquad (10)$$

where

$$\Delta E_{A_1 A_2}^{\text{bh}} = E_{A_1}^{\text{bh}} - E_{A_2}^{\text{bh}}, \qquad (11)$$

and the ratio of the C coefficients is denoted by

$$\alpha_{A_1 A_2} = C_{A_1,Z_1,H}/C_{A_2,Z_2,H}. \qquad (12)$$

We see that the double ratio depends only on the temperature of the system and the difference between the hyperon separation energies of the fragments. We can also control a small uncertainty coming from the Coulomb interaction of fragments in the freeze-out (see below Sec. III B).

One can simply deduce from Eq. (10) that the logarithm of the double ratio is directly proportional to the difference of the hyperon binding energies in A_1 and A_2 hypernuclei, $\Delta E_{A_1 A_2}^{\text{bh}}$, divided by temperature. Therefore, we can finally

rewrite the relation between the hypernuclei yields and the hyperon binding energies as

$$\Delta E_{A_1 A_2}^{\mathrm{bh}} = T \cdot \left[\ln\left(\alpha_{A_1 A_2}\right) - \ln\left(DR_{A_1 A_2}\right) \right]. \quad (13)$$

Sometimes we expect a large difference in hyperon binding energies of both involved nuclei. For example, according to the liquid-drop approach [see Eq. (2)], it can happen when the difference between A_1 and A_2 is considerable (i.e., the mass number A_2 is much larger than A_1). The influence of the preexponential $\alpha_{A_1 A_2}$ coefficients is small and it can be directly evaluated depending on the selected hypernuclei. This opens a possibility for the explicit determination of the binding energy difference from the yields measured in the experiments. Within this method, it is necessary to measure a certain number of the hypernuclei in one reaction and select the corresponding pairs of hypernuclei. One has to identify such hypernuclei, for example, by the correlations and vertex technique. However, there is no need to measure very precisely the momenta of all particles produced in the reaction (including after the week decay of hypernuclei) to obtain their binding energy, as it must be done if one use direct processes of the hyperon capture in the ground and slightly excited states of the target nuclei (e.g., in missing mass experiments [2,33]). Therefore, our procedure perfectly suits for investigation of hypernuclei in the high-energy deep-inelastic hadron- and ion-induced reactions.

B. Application of the method

It is clear from Sec. III A that the suggested double ratio approach can be applied to hypernuclei with any number of hyperons. Obviously, Eqs. (1), (10), and (13) can be used for $H > 1$. In heavy-ion nuclear reactions one can obtain a multistrange residues with a quite large probability [19], and a very wide mass/isospin range will be available for examination. As a result, one can get direct experimental evidences for hyperon binding energies in double/triple hypernuclei and on influence of the isospin on hyperon interactions in multihyperon nuclear matter.

The connection between the relative hyperon binding energies $\Delta E_{A_1 A_2}^{\mathrm{bh}}$ and their absolute values can be done straightforwardly such that it will be sufficient to make normalization to the binding energy of a known hypernuclei (e.g., A_2) obtained with other methods. However, even relative values are extremely important, when we pursue a goal to investigate the trends of the hyperon interaction in exotic nuclear surroundings, e.g., neutron-rich or neutron-poor ones, and investigate multistrange hypernuclei.

To illustrate the last point in Fig. 1, we present the dependence of the difference in hyperon binding energies $\Delta E_{A_1 A_2}^{\mathrm{bh}}$ (the notation is shortened to ΔE_{bh}) divided by the temperature, versus $\Delta A = A_2 - A_1$ the mass number difference of the isotopes. The calculations were performed with the hyper-SMM version (see Refs. [5,15]) outlined in Sec. II, for the system with baryon number $A_0 = 200$, charge $Z_0 = 80$, and containing $H_0 = 4$ Λ hyperons. The formulas (10) and (13) are applied to extract this difference. We have plotted nine various double ratios of isotopes by suggesting hyper-^{13}C nucleus as A_1. Other
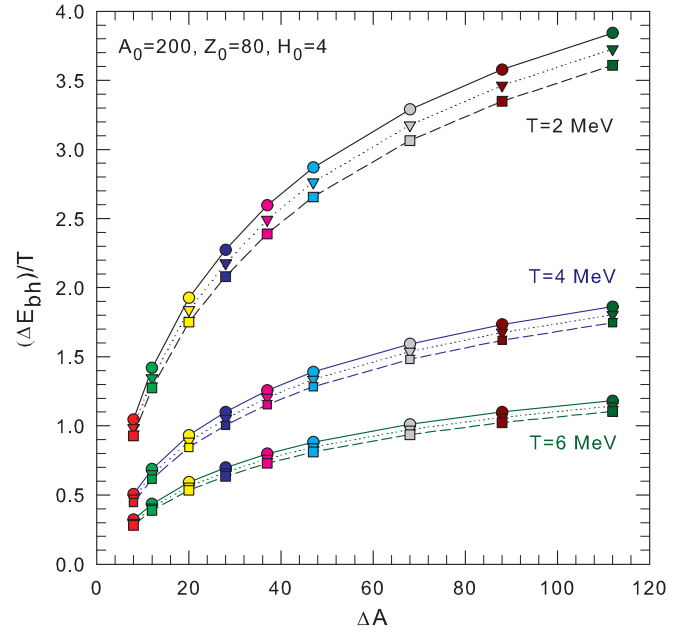
FIG. 1. The difference of binding energies of hyperons in nuclei extracted from the double yield ratio (ΔE_{bh}) divided by the temperature T versus the mass number difference of these nuclei ΔA, as calculated with the statistical model at different temperatures relevant for multifragmentation reactions. Baryon composition and temperatures (for groups of curves) of the initial system are given in the figure. The results for involved isotopes (see the text) are demonstrated by different color symbols connected with lines, where circles (solid lines) are for single hypernuclei, inverse triangles (dotted lines) are for double hypernuclei, squares (dashed lines) are for triple hypernuclei.

nuclei ($A_2 = 21$, 25, 33, 41, 50, 60, 81, 101, 125) are selected in order to provide a broad and representative range of ΔA. In particular, we consider the yield ratios of $^{21}\mathrm{O}_{H\Lambda}/^{20}\mathrm{O}_{(H-1)\Lambda}$, $^{25}\mathrm{Mg}_{H\Lambda}/^{24}\mathrm{Mg}_{(H-1)\Lambda}$, $^{33}\mathrm{P}_{H\Lambda}/^{32}\mathrm{P}_{(H-1)\Lambda}$, $^{41}\mathrm{S}_{H\Lambda}/^{40}\mathrm{S}_{(H-1)\Lambda}$, $^{50}\mathrm{Ca}_{H\Lambda}/^{49}\mathrm{Ca}_{(H-1)\Lambda}$, $^{60}\mathrm{Cr}_{H\Lambda}/^{59}\mathrm{Cr}_{(H-1)\Lambda}$, $^{81}\mathrm{Ge}_{H\Lambda}/^{80}\mathrm{Ge}_{(H-1)\Lambda}$, $^{101}\mathrm{Zr}_{H\Lambda}/^{100}\mathrm{Zr}_{(H-1)\Lambda}$, $^{125}\mathrm{Sn}_{H\Lambda}/^{124}\mathrm{Sn}_{(H-1)\Lambda}$, to $^{13}\mathrm{C}_{H\Lambda}/^{12}\mathrm{C}_{(H-1)\Lambda}$, where $H = 1$, 2, 3. We investigate the sensitivity of our results to the primary excitation of the system by assuming temperatures $T = 2$, 4, and 6 MeV, which cover the expected temperature range in fragmentation and multifragmentation reactions. One can see that the extracted $\Delta E_{\mathrm{bh}}/T$ increases regularly with ΔA, as follows from the hyperterm (7) adopted in the model. It is interesting that in our case this difference in the multistrange hypernuclei is close to single hypernuclei. This is an obvious consequence of the model formula for hyperons in nuclei. Naturally, this function might be another one reflecting modified hyperon binding energies, and it could be investigated via the double ratios from experimental data. In such a way we can get also an interesting possibility to improve phenomenological formulae for hypernuclei according to the observed trends.

If we take into account the temperature we can get very instructive curves of ΔE_{bh} versus ΔA shown in Fig. 2. For simplicity, only the results obtained via double ratio of single
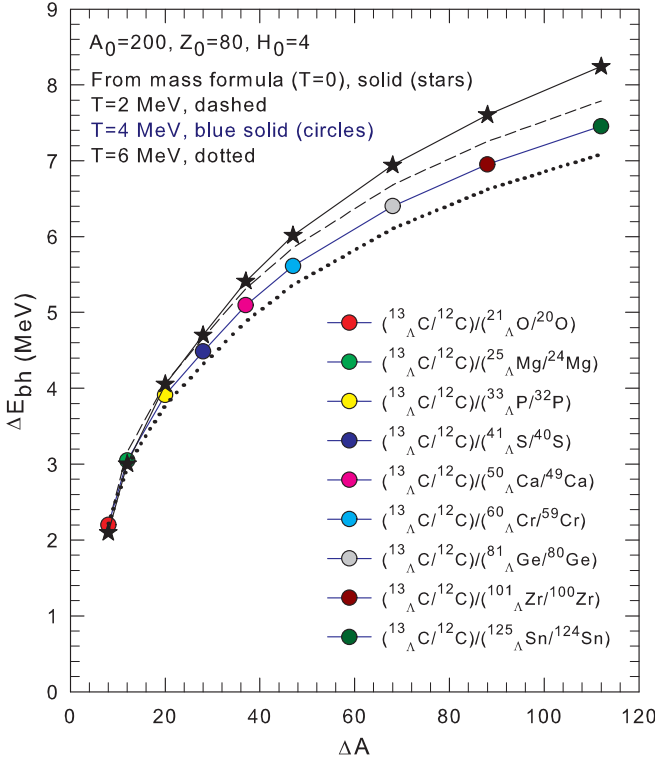
FIG. 2. The difference of binding energies of hyperons in nuclei (ΔE_{bh}) versus the mass number difference of these nuclei ΔA for single hypernuclei. The statistical calculations are performed involving the double ratio yields shown in the figure for temperatures $T = 2$ MeV (dashed line), 4 MeV (thin solid line, circle symbols), and 6 MeV (dotted line). The stars (thick solid line) are the direct calculation of ΔE_{bh} according to the adopted hyperfragment formula (2)–(7) at $T = 0$ and $V \to \infty$. The initial parameter of the hypernuclear system are as in Fig. 1.

hypernuclei and normal nuclei are shown. However, as is clear from Fig. 1 an involvement of multiple hypernuclei lead to similar trends. The demonstrated regularities are again obviously consistent with the adopted hypermass formula (see also Fig. 1 in Ref. [5]). For a detailed comparison, with the solid dark curve connecting the star symbols we show the results for the differences in hyperon binding energies of the selected isotopes obtained directly from this mass formula. One can see within SMM that by decreasing temperature we approach the real formula values. The physical reason of the deviations is in the temperature corrections of the bulk and surface fragment energies (in the liquid-drop approximation, see Sec. II). Nevertheless, they decrease with temperature and are under control in the model. Another reason for the deviation is the Coulomb interaction of fragments in the freeze-out volume, see formula (6). The Coulomb term influences the fragment yields and their double ratios, especially if large fragments are involved. In the model, when we increase this volume our results for small T become very close to the mass formula ones. The results at all temperatures are regular and close to each other within 10%, and this gives us a confidence that the method is reliable.

The comprehensive analysis of double hypernuclei and multihyperon nuclei is possible within this approach, and it

seems a realistic way to address experimentally the hyperon binding also in multistrange nuclei. This is an important advantage over the standard hypernuclear measurements. Actually, the disintegration of hot hyperresidues best suits this analysis since all kinds of normal and hyperfragments can be formed within the same statistical process. As was previously established in multifragmentation studies [34,35], the selection of adequate reaction conditions can be experimentally verified.

IV. APPROXIMATION OF COLD FRAGMENTS IN THE FREEZE-OUT STATE

In the first statistical approaches, the production of final (cold) fragments in the freeze-out volume were considered (see, e.g., Ref. [36]). In this case the sophisticated description of the hot fragments is omitted, and we consider only fixed fragment binding energies without a temperature dependence. This physical condition may still be adequate for the formation of lightest fragments in the high-energy nuclei collisions with a large energy deposition. Then, after disintegration of nuclear systems, the grand-canonical yields of a normal nucleus in the ground state can be written as

$$Y_{A,Z} = g_{A,Z} \cdot V_f \frac{A^{3/2}}{\lambda_T^3} \exp\left[-\frac{1}{T}\left(E_{A,Z}^b - \mu_{A,Z}\right)\right],$$
$$\mu_{A,Z} = A\mu + Z\nu, \tag{14}$$

where A, Z are the nucleon number and charge, $g_{A,Z}$ is the standard spin factor, and $E_{A,Z}^b$ is the nucleus ground-state binding energy.

It is obvious that this case can be easy generalized for hypernuclei, with the same expression (1), if we take into account the binding energy of hyperons and introduce the total (temperature independent) nucleus binding energy $E_{A,Z,H}^b$ instead of $F_{A,Z,H}$. Then all our formulas (8)–(12) remain similar to the standard multifragmentation, however, with new spin factors. In particular, the relation (13) can be also used for evaluation of the hyperon binding energy from the hypernuclei yields.

Isobar double ratios

Another interesting method for this study is to use the double ratios of yields with the same mass numbers for light and heavy pairs. This case is easy to illustrate for cold fragments. The so-called strangeness population factor S was introduced in Ref. [37] for interpretation of light hypernuclei production in relativistic heavy-ion collision (at momenta of 11.5 A GeV/c):

$$S = \frac{Y_{^3H_\Lambda}/Y_{^3He}}{Y_\Lambda/Y_P}. \tag{15}$$

Generally, if we involve the pairs of nuclei which differ by one proton instead of Λ hyperon, we can write the isobar double ratio:

$$DR_{A_1A_2}^I = \frac{Y_{A_1,Z_1,H}/Y_{A_1,Z_1+1,H-1}}{Y_{A_2,Z_2,H}/Y_{A_2,Z_2+1,H-1}} = \alpha_{A_1A_2}^I \exp\left[-\frac{1}{T}\left(\Delta E_X^b\right)\right], \tag{16}$$

where

$$\alpha_{A_1 A_2}^I = \frac{g_{A_1, Z_1, H} / g_{A_1, Z_1+1, H-1}}{g_{A_2, Z_2, H} / g_{A_2, Z_2+1, H-1}}, \qquad (17)$$

and the binding energy difference between four fragments

$$\Delta E_X^{\mathrm{b}} = \left(E_{A_1, Z_1, H}^b - E_{A_2, Z_2, H}^b \right) \\ - \left(E_{A_1, Z_1+1, H-1}^b - E_{A_2, Z_2+1, H-1}^b \right). \qquad (18)$$

The expression (16) can not be factorized into the parts related to the binding energies of nuclei with A_1 and A_2 and the parts related only to the hyperon binding energy [as it was possible by using the formula (8)], since it includes also the difference of the hyperon energy in hypernuclei with $Z + 1$. Therefore, such an extraction of the hyperon binding energy would require a complicated solution of the coupled equations and extra experimental isobar measurements. Still, the convenient application of DR^I can be found for single hypernuclei with $H = 1$, when there are only normal nuclei (at $H - 1 = 0$ and $Z + 1$) with known binding energies as the pair nuclei. In this case one can rewrite the formula (13) as

$$\Delta E_{A_1 A_2}^{\mathrm{bh}} = T \cdot \left[\ln \left(\alpha_{A_1 A_2}^I \right) - \ln \left(DR_{A_1 A_2}^I \right) \right] + \Delta E_{A_1 A_2}^{\mathrm{GS}}, \quad (19)$$

where $\Delta E_{A_1 A_2}^{\mathrm{GS}}$ is the difference of the ground-state binding energies of nonstrange nuclei:

$$\Delta E_{A_1 A_2}^{\mathrm{GS}} = \left(E_{A_1, Z_1+1}^b - E_{A_2, Z_2+1}^b \right) - \left(E_{A_1-1, Z_1}^b - E_{A_2-1, Z_2}^b \right). \tag{20}$$

In the above-mentioned example, as was obtained by AGS-E864 collaboration [37], we have $S = 0.36$ (with large error bars $+ - 0.26$) for the most central collisions and for fragments produced in the midrapidity region. Since the binding energies of all nuclei in S factor (15) are known from other experiments we can evaluate from formula (16), the temperature of the excited hypersource leading to production of these fragments and hypernuclei. The found chemical temperature is around $T \approx 5.5$ MeV. This is typical for the nuclear liquid-gas phase coexistence region in nuclear finite systems under the condition that all available baryons are produced in dynamical nucleon collisions inside nuclei. It is also consistent with the limited equilibrium of fragments reported previously for central heavy-ion collisions [38].

V. PARAMETERS AND PROCESSES FOLLOWING THE STATISTICAL FRAGMENTATION

The conception of the statistical formation of fragments in the freeze-out volume suggests the existence of important parameters, such as the temperature. In addition, the primary fragments may be excited and it suggests some phenomena, as secondary processes, which can finally change the baryon composition of fragments after they leave the freeze-out volume. All these effects were under careful examination previously in multifragmentation reactions in normal nuclei. We outline how it could be taken into account in the hypernuclear case.
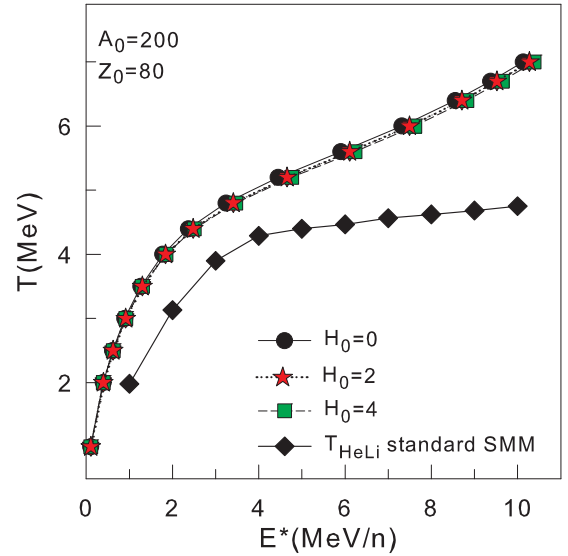
FIG. 3. The temperature versus the excitation energy for the disintegration of the hypernuclear system with parameters given in the figure. The statistical calculations including different initial numbers of hyperons (0, 2, and 4) are shown by different symbols and lines. (For better view the symbols are shifted slightly along the horizontal axis being at the same E^*.) The helium-lithium isotope temperature (see the text) calculated within the standard multifragmentation model are represented by diamonds.

A. Temperature and the freeze-out state

In order to extract $\Delta E_{A_1 A_2}^{\mathrm{bh}}$ from experiments within the double ratio approach, we should determine the temperature T of the disintegrating hypernuclear system. This quantity was under intensive investigation in recent years in connection with multifragment formation. There were various suggested methods such as using the kinetic energies of fragments, excited states population, and isotope thermometers [28,39,40]. Usually, all evaluations give the temperature around 4–6 MeV in the very broad range of the excitation energies (at $E^* > 2-3$ MeV per nucleon), providing so-called a plateaulike behavior of the caloric curve [24,28]. The isotope thermometer method is the most promising, since it allows for involving a large number of normal measured isotopes in the same reactions, which produce hypernuclei. The corresponding experimental and theoretical research were performed in previous years to investigate better the temperature and isospin dependence of the nuclear liquid-gas type phase transition [40–43].

In Fig. 3 we show the caloric curve (the temperature versus the excitation energy) for the nuclear system with the mass number of 200 and the charge of 80. The calculations were done in the framework of the above formulated statistical model [5,15]. The cases with the initial hyperon numbers of 0, 2, and 4 are considered. One can see that a small hyperon admission in the system does not change practically the caloric curve, but only the temperature becomes a little bit lower. We have calculated also the so-called helium-lithium temperature (T_{HeLi}) within the normal multifragmentation model. Similarly, we expect a negligible

variation of the He and Li yields, and their yield ratios, caused by the small hyperon admission. This temperature was found from the standard prescription for isotope yields as it was suggested in Ref. [28], and as performed in many other works. Such an isotope temperature follows quite reasonably the normal temperature in the most important fragment production region of excitation energy from 2–6 MeV per nucleon. Therefore, the correction with 20% to 30% T_{HeLi} can be used for the determination of temperatures in the systems.

In addition to measuring isotopes and hyper-isotopes it would be instructive to select the reaction conditions leading to similar multifragmentation freeze-out states. The freeze-out restoration methods were extensively tested previously. In particular, the masses and excitation energies of the hypernuclear residues can be found with a sufficient precision within the methods developed in Refs. [34,35]. In the future one can analyze the subsequent ranges of the excitation energy of sources (from low to very high ones) to investigate the evolution of the hypernuclei with the temperature and the phase transition in hypermatter. It is especially interesting to move into the neutron-rich domain of the nuclear chart, by selecting neutron-rich target or projectiles.

B. Secondary deexcitation corrections

In many physical cases, the final fragments can be considered as produced statistically in the freeze-out volume. However, taking into account the experience accumulated for the nuclear reactions so far, we may expect that the primary fragments and hyperfragments (especially large ones) formed in the freeze-out are excited. Therefore, they will quickly decay after escaping the freeze-out stage. For low excited sources this fragment excitation energy should roughly correspond to the compound nucleus temperature. As was established in theory and multifragmentation experiments [44], the internal fragment excitations can reach around 2 MeV per nucleon and even more if the residue sources are highly excited. The secondary deexcitation influences all four fragments entering the double ratio and the fragments will lose few nucleons. Previous investigations of similar nuclear decay processes of excited nuclei in normal multifragmentation reactions tell us that this is a process of the continuous modification of initial (mother) nuclei into final (daughter) ones by emitting particles [24]. Following this deexcitation the mass numbers will change and we expect a smooth transformation of $\Delta E^{\text{bh}}_{A_1 A_2}$ versus the variation of mass difference $\Delta A = (A_2 - A_1)$. Therefore, modified yields and mass numbers should be possible to use for the final estimate.

In order to evaluate this effect we have adopted the nuclear evaporation model generalized for hypernuclei, which was developed in Ref. [45]. In this case, the fragments at the freeze-out are described as discussed in Sec. II. It was demonstrated in Ref. [45] that mostly neutrons and other light normal particles will be emitted from hot large hyperfragments, since the hyperons have a larger binding energy. In Figs. 4 and 5 we show how the secondary deexcitation can modify the results on $\Delta E^{\text{bh}}_{A_1 A_2}$ (in the figures noted again as ΔE_{bh}) versus ΔA, corresponding to single and double hypernuclei. For clarity
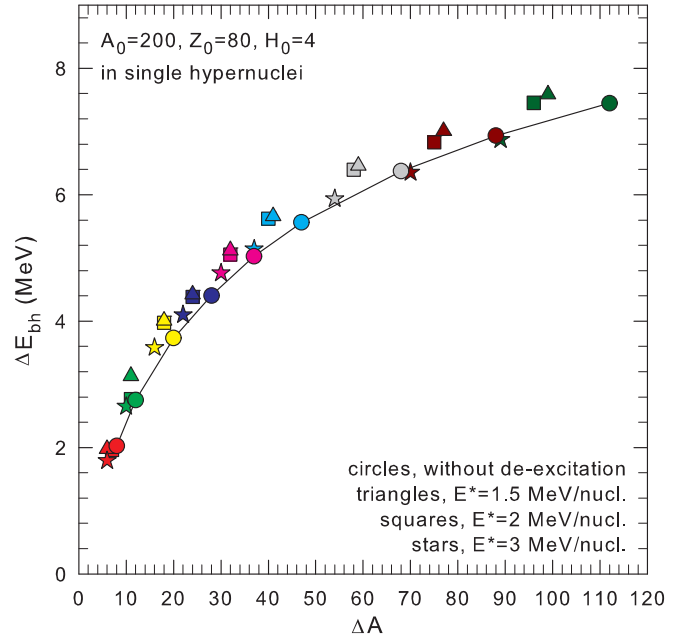
FIG. 4. Influence of the secondary deexcitation on the difference of binding energies of hyperons in nuclei ΔE_{bh} as function of their mass number difference ΔA, by taking single hypernuclei (which are the same as in Fig. 2). The calculations of double ratio yields for primary hot nuclei are shown for temperature 4 MeV (solid line, color circle symbols). The triangles, squares, and stars stand for the calculations with modified double ratios after the secondary deexcitation (via nuclear evaporation) of primary nuclei at excitation energies of 1.5, 2.0, and 3.0 MeV/nucleon, respectively. The same color symbols show the modification of ΔE_{bh} and ΔA after the deexcitation evolution of many nuclei leading to the same daughter ones (see the text).

we use the same mother nuclei as presented in Figs. 1 and 2, which are noted in Sec. III B. The typical temperature of $T = 4$ MeV is taken for initial fragment yields to be consistent with the previous figures. As seen in Fig. 2, the results obtained from double ratios of primary yields of nuclei change very little with variation of the temperature in the multifragmentation region. The realistic values of internal excitation energies of these fragments, $E^* = 1.5$ per nucleon (a low value), 2 MeV per nucleon (a most likely value from experimental data [44]), and $E^* = 3$ MeV per nucleon were assumed. The last value is the highest estimate taken to investigate the trend caused by the secondary process. In the beginning we have calculated which daughter nuclei can be produced after the evaporation by taking into account their maximum yield. In this case, for example, after deexcitation of ^{12}C, ^{13}C$_\Lambda$, ^{124}Sn, and ^{125}Sn$_\Lambda$ at $E^* = 3$ MeV/nucleon we obtain ^{10}B, ^{11}B$_\Lambda$, ^{99}Pd, and ^{100}Pd$_\Lambda$ nuclei, respectively. As we know the same daughter nuclei can be produced after evaporation of other nuclei close to A and Z. We have also calculated the deexcitation of such nuclei, that their numbers may reach few tens at the highest excitation energy. We have taken into account the weight of all primary nuclei after multifragmentation in the freeze-out volume and evaluated their contribution in the final daughter yield. Afterward, according to the formula (13) we found new
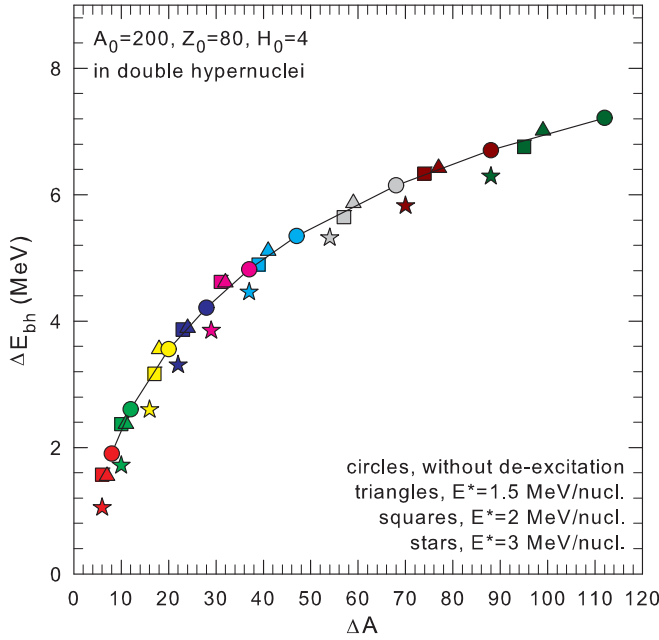
FIG. 5. The same as in Fig. 4, however, for double hypernuclei (see the text).

ΔE_{bh}. In the figures the results of the calculations including the evaporation are given by triangle, square, and star symbols corresponding to the above-mentioned internal excitations.

To see clearly the general transformation of the initial function, in Figs. 4 and 5 the values of ΔA and ΔE_{bh} are shown with the same color symbols for the mother and daughter isotopes. This connection can also be seen by the corresponding groups in the ΔA axis, so that after evaporation there is a regular shift of ΔA values to smaller ones as a result of nucleon losses. This can be distinguished by comparing the primary circles with the triangles, squares, and stars. This shift is especially prominent in big nuclei because of their total excitation energies are higher. There are also modifications of ΔE_{bh} because of the isotope yield variations.

Finally, after the secondary processes and the sum of all contributions the whole curve of ΔE_{bh} versus ΔA may look shifted a little bit. We see that the deexcitation influence on ΔE_{bh} values is rather moderate (the uncertainty is within 10%). The reason is that after the evaporation calculations the yield ratios change small. As well known, the nuclei initially close to A and Z are deexcited similarly. Also, the involvement of the nuclei neighboring to primary ones does smooth the possible fluctuations of the final yield, which can occur in the case of separate nuclei. However, the general form of this dependence does not change. In our case ($T = 4$ MeV) the interesting effect is a noticeable decrease of extracted ΔE_{bh} with increasing excitation energy. This is related to the production of light primary fragments that contribute to the $13C_{H\Lambda}/12C_{(H-1)\Lambda}$ ratio in the numerator of the double ratio [Eq. (10)]. The yield distributions of light fragments with H hyperons in multifragmentation increase faster with A than for fragments with H-1 hyperons [5,15]. That leads to

moderate increasing the averaged yield ratio for the light isotope pair.

If the freeze-out conditions were precisely known from the analyses of experiments the model calculations could be used for an adequate corrections of the experimentally extracted ΔE_{bh}. It is similar to the procedures elaborated previously, such as the evaluation of the isotope temperatures in normal multifragmentation studies [28]. We conclude from the Figs. 4 and 5 that the initial difference in hyperon binding energies of hypernuclei can be extracted by generating similar plots even after the secondary deexcitation.

VI. CONCLUSION

During the last six decades there has been a permanent increase in the number of measured hypernuclei with their binding energies. However, the progress is slow such that the traditional hypernuclear methods (e.g., involving the missing mass spectroscopy) can address only a small number of isotopes, due to the special requirements on targets in hadron- and lepton-induced reactions. Also the development of the detectors for measuring practically all produced particles with their exact kinetic energies is very expensive and not always practical, which makes problems for a desirable acceleration of the studies.

The suggested double ratio method is related to deep inelastic reactions producing all kinds of hypernuclei with sufficiently large cross sections in the multifragmentation process. This is a typical case for relativistic ion-ion and hadron-ion collisions. Only the identification of hypernuclei is required, and, as demonstrated in recent ion experiments, there are effective ways to perform it. The experimental extraction of the difference between the hyperon binding energies for hypernuclei ($\Delta E^{\mathrm{bh}}_{A_1 A_2}$) via their yields is a novel and practical way to pursue hypernuclear studies. The advantage of this method over the traditional hypernuclear ones is that the exact determination of all produced particle parameters (with their decay products) is not necessary, and only the relative measurements are necessary for this purpose. Therefore, for comparison of various hypernuclei one can use similar weak-decay chains and their products. For example, if we take the pairs of the large hyper-isotopes, they undergo weak decay in a nonmesonic channel that can be found by products far from the collision point with the vertex technique. The correlation between the produced isotopes and particles is adequate information for the double ratio method.

It is even more interesting and important that one can also determine the difference of hyperon binding energies in double and multihypernuclei within this method. This gives an access to hyperon-hyperon interactions and properties of multihyperon matter. It is very difficult to measure the hyperon binding energies for exotic (neutron-rich and neutron-poor) nuclear species within traditional hypernuclear experiments. On the other hand, the hypernuclei with extreme isospin can be easily obtained in relativistic fragmentation reactions. Most of them may have the statistical origin and the suggested method opens an effective way for extension of the hypernuclear chart. We believe that novel conclusions can be obtained for neutron-rich and neutron-poor hypernuclei with the double

ratio method. The isospin influence on the hyperon interactions in matter (revealing in the hyperon binding energies) will be possible to extract directly from experimental data. Especially, multistrange nuclear systems would be interesting, since they can give info on evolution of the hyperon-hyperon interaction depending on strangeness. These measurements are important for many astrophysical sites, for example, for understanding the neutron star structure [46,47].

Such kinds of research may be possible at the new generation intermediate energy ion accelerator facilities such as FAIR (Darmstadt), NICA (Dubna), and others. Hopefully, the new advanced experimental installations for the fragment detection will be available soon [48,49].

[1] H. Bando, T. Mottle, and J. Zofka, Int. J. Mod. Phys. A **5**, 4021 (1990).

[2] O. Hashimoto and H. Tamura, Prog. Part. Nucl. Phys. **57**, 564 (2006).

[3] J. Schaffner, C. B. Dover, A. Gal, C. Greiner, and H. Stoecker, Phys. Rev. Lett. **71**, 1328 (1993).

[4] Special issue on *Progress in Strangeness Nuclear Physics*, edited by A. Gal, O. Hashimoto, and J. Pochodzalla, Nucl. Phys. A **881**, 1 (2012).

[5] N. Buyukcizmeci, A. S. Botvina, J. Pochodzalla, and M. Bleicher, Phys. Rev. C **88**, 014611 (2013).

[6] T. Hell and W. Weise, Phys. Rev. C **90**, 045801 (2014).

[7] M. Danysz and J. Pniewski, Philos. Mag. **44**, 348 (1953).

[8] The STAR collaboration, Science **328**, 58 (2010).

[9] B. Dönigus *et al.* (ALICE collaboration), Nucl. Phys. A **904-905**, 547c (2013).

[10] The PANDA collaboration, http://www-panda.gsi.de; and arXiv:physics/0701090.

[11] I. Vassiliev *et al.* (CBM collaboration), JPS Conf. Proc. **17**, 092001 (2017).

[12] T. R. Saito *et al.* (HypHI collaboration), Nucl. Phys. A **881**, 218 (2012).

[13] https://indico.gsi.de/event/superfrs3 (access to pdf files via timetable and key 'walldorf').

[14] NICA White Paper, http://theor.jinr.ru/twiki-cgi/view/NICA/WebHome; http://nica.jinr.ru/files/BM@N

[15] A. S. Botvina and J. Pochodzalla, Phys. Rev. C **76**, 024909 (2007).

[16] A. S. Botvina, K. K. Gudima, J. Steinheimer, M. Bleicher, and I. N. Mishustin, Phys. Rev. C **84**, 064904 (2011).

[17] A. S. Botvina, K. K. Gudima, and J. Pochodzalla, Phys. Rev. C **88**, 054605 (2013).

[18] A. S. Botvina *et al.*, Phys. Lett. B **742**, 7 (2015).

[19] A. S. Botvina, K. K. Gudima, J. Steinheimer, M. Bleicher, and J. Pochodzalla, Phys. Rev. C **95**, 014902 (2017).

[20] Z. Rudy, W. Cassing *et al.*, Z. Phys. A **351**, 217 (1995).

[21] Th. Gaitanos, H. Lenske, and U. Mosel, Phys. Lett. B **675**, 297 (2009).

[22] T. A. Armstrong, J. P. Bocquet, G. Ericsson, T. Johansson, T. Krogulski, R. A. Lewis, F. Malek, M. Maurel, E. Monnand, J. Mougey, H. Nifenecker, J. Passaneau, P. Perrin, S. M. Polikanov, M. Rey-Campagnolle, C. Ristori, G. A. Smith, and G. Tibell, Phys. Rev. C **47**, 1957 (1993).

[23] H. Ohm, T. Hermes, W. Borgs, H. R. Koch, R. Maier, D. Prasuhn, H. J. Stein, O. W. B. Schult, K. Pysz, Z. Rudy, L. Jarczyk, B. Kamys, P. Kulessa, A. Strzalkowski, W. Cassing, Y. Uozumi, and I. Zychor, Phys. Rev. C **55**, 3062 (1997).

[24] J. P. Bondorf, A. S. Botvina, A. S. Iljinov, I. N. Mishustin, and K. Sneppen, Phys. Rep. **257**, 133 (1995).

[25] H. Xi *et al.*, Z. Phys. A **359**, 397 (1997).

[26] K. Turzo *et al.*, Eur. Phys. J. A **21**, 293 (2004).

[27] R. P. Scharenberg, B. K. Srivastava, S. Albergo, F. Bieser, F. P. Brady, Z. Caccia, D. A. Cebra, A. D. Chacon, J. L. Chance, Y. Choi, S. Costa, J. B. Elliott, M. L. Gilkes, J. A. Hauger, A. S. Hirsch, E. L. Hjort, A. Insolia, M. Justice, D. Keane, J. C. Kintner, V. Lindenstruth, M. A. Lisa, H. S. Matis, M. McMahan, C. McParland, W. F. J. Muller, D. L. Olson, M. D. Partlan, N. T. Porile, R. Potenza, G. Rai, J. Rasmussen, H. G. Ritter, J. Romanski, J. L. Romero, G. V. Russo, H. Sann, A. Scott, Y. Shao, T. J. M. Symons, M. Tincknell, C. Tuve, S. Wang, P. Warren, H. H. Wieman, T. Wienold, and K. Wolf, Phys. Rev. C **64**, 054602 (2001).

[28] J. Pochodzalla, Prog. Part. Nucl. Phys. **39**, 443 (1997).

[29] R. Ogul *et al.*, Phys. Rev. C **83**, 024608 (2011).

[30] W. Greiner, Int. J. Mod. Phys. E **5**, 1 (1995).

[31] C. Samanta *et al.*, J. Phys. G: **32**, 363 (2006).

[32] A. S. Botvina, M. Bleicher, and N. Buyukcizmeci, arXiv:1711.01159.

[33] A. Esser, S. Nagao, F. Schulz, P. Achenbach, C. AyerbeGayoso, R. Bohm, O. Borodina, D. Bosnar, V. Bozkurt, L. Debenjak, M. O. Distler, I. Friscic, T. Fujii, T. Gogami, O. Hashimoto, S. Hirose, H. Kanda, M. Kaneta, E. Kim, Y. Kohl, J. Kusaka, A. Margaryan, H. Merkel, M. Mihovilovic, U. Muller, S. N. Nakamura, J. Pochodzalla, C. Rappold, J. Reinhold, T. R. Saito, A. SanchezLorente, S. SanchezMajos, B. S. Schlimme, M. Schoth, C. Sfienti, S. Sirca, L. Tang, M. Thiel, K. Tsukada, A. Weber, and K. Yoshida, Phys. Rev. Lett. **114**, 232501 (2015).

[34] L. Pienkowski, K. Kwiatkowski, T. Lefort, W.-c. Hsi, L. Beaulieu, V. E. Viola, A. Botvina, R. G. Korteling, R. Laforest, E. Martin, E. Ramakrishnan, D. Rowland, A. Ruangma, E. Winchester, S. J. Yennello, B. Back, S. Gushue, and L. P. Remsberg, Phys. Rev. C **65**, 064606 (2002).

[35] S. N. Soisson *et al.*, J. Phys. G: Nucl. Part. Phys. **39**, 115104 (2012).

[36] M. N. Saha, Proc. R. Soc. A **99**, 135 (1921).

[37] T. A. Armstrong, K. N. Barish, S. Batsouli, S. J. Bennett, M. Bertaina, A. Chikanian, S. D. Coe, T. M. Cormier, R. Davies, C. B. Dover, P. Fachini, B. Fadem, L. E. Finch, N. K. George, S. V. Greene, P. Haridas, J. C. Hill, A. S. Hirsch, R. Hoversten, H. Z. Huang, H. Jaradat, B. S. Kumar, T. Lainis, J. G. Lajoie, R. A. Lewis, Q. Li, B. Libby, R. D. Majka, T. E. Miller, M. G. Munhoz, J. L. Nagle, I. A. Pless, J. K. Pope, N. T. Porile, C. A. Pruneau, M. S. Z. Rabin, J. D. Reid, A. Rimai, A. Rose, F. S. Rotondo, J. Sandweiss, R. P. Scharenberg, A. J. Slaughter, G. A. M. L. Tincknell, W. S. Toothacker, G. VanBuren, F. K. Wohn, and Z. Xu, Phys. Rev. C **70**, 024902 (2004).

[38] W. Neubert and A. S. Botvina, Eur. Phys. J. A **17**, 559 (2003).

[39] J. P. Bondorf, A. S. Botvina, and I. N. Mishustin, Phys. Rev. C **58**, R27 (1998).

[40] A. Kelic, J. B. Natowitz, and K.-H. Schmidt, Eur. Phys. J. A **30**, 203 (2006).

[41] V. E. Viola *et al.*, Nucl. Phys. A **681**, 267c (2001).

[42] R. Ogul and A. S. Botvina, Phys. Rev. C **66**, 051601(R) (2002).

[43] N. Buyukcizmeci *et al.*, Eur. Phys. J. A **25**, 57 (2005).

[44] S. Hudan, A. Chbihi, J. D. Frankland, A. Mignon, J. P. Wieleczko, G. Auger, N. Bellaize, B. Borderie, A. Botvina, R. Bougault, B. Bouriquet, A. M. Buta, J. Colin, D. Cussol, R. Dayras, D. Durand, E. Galichet, D. Guinet, B. Guiot, G. Lanzalone, P. Lautesse, F. Lavaud, J. F. Lecolley, R. Legrain, N. LeNeindre, O. Lopez, L. Manduci, J. Marie, L. Nalpas, J. Normand, M. Parlog, P. Pawlowski, M. Pichon, E. Plagnol, M. F. Rivet, E. Rosato, R. Roy, J. C. Steckmeyer, G. Tabacaru, B. Tamain, A. vanLauwe, E. Vient, M. Vigilante, and C. Volant, Phys. Rev. C **67**, 064613 (2003).

[45] A. S. Botvina, N. Buyukcizmeci, A. Ergun, R. Ogul, M. Bleicher, and J. Pochodzalla, Phys. Rev. C **94**, 054615 (2016).

[46] J. Schaffner-Bielich, Nucl. Phys. A **804**, 309 (2008).

[47] H. Togashi, E. Hiyama, Y. Yamamoto, and M. Takano, Phys. Rev. C **93**, 035808 (2016).

[48] Th. Aumann, Progr. Part. Nucl. Phys. **59**, 3 (2007).

[49] H. Geissel *et al.*, Nucl. Inst. Meth. Phys. Res. B **204**, 71 (2003).